# Enhanced fabrication of silicon carbide membranes for wastewater treatment: From laboratory to industrial scale

Esra Eray [a,b], Vittorio Boffa [b], Mads K. Jørgensen [b], Giuliana Magnacca [c], Victor M. Candelario [a,*]

[a] *Liqtech International A/S, Industriparken 22C, DK-2750, Ballerup, Denmark*
[b] *Department of Chemistry and Bioscience, Center of Membrane Technology, Aalborg University, Fredrik Bajers Vej 7H, DK-9220, Aalborg Øst, Denmark*
[c] *Department of Chemistry and NIS Interdepartmental Centre, University of Turin, Via P. Giuria 7, 10125, Turin, Italy*

## ARTICLE INFO

## ABSTRACT

An environmental-friendly procedure has been developed for the fabrication of pure silicon carbide membranes on macroporous SiC support via ceramic processing. Water dispersions of α-SiC powders were used for deposition of membrane layers by dip-coating. The influence of the fine/coarse powder mixing ratio, solid loading, use of α-SiC powders with different particle sizes as well as sintering temperature on the structural morphology of the membranes were investigated in order to obtain uniform, homogeneous, and defect-free SiC membrane layers. The optimized protocol was up-scaled on industrial SiC tubular supports with high reproducibility, reducing the sintering temperature compared to conventional SiC membrane synthesis. The new SiC membranes were used for the treatment of a secondary effluent from Biofos wastewater treatment plant in Avedøre, Denmark, and their performances evaluated in terms of removal of the suspended solids, colloidal particles and reduction of chemical oxygen demand. According to filtration results, the new SiC membranes showed high removal of suspended solids (99.4%) and colloidal particles (96%) along with significant reduction of chemical oxygen demand (83%). The pure SiC membranes developed in this study have a potential to be applied in the wastewater treatment since they combine the robustness of SiC with high selectivity.

## 1. Introduction

Purification and reuse of water from secondary effluents are becoming an attractive solution for the ever-increasing water scarcity and water quality deterioration issues. Secondary effluents from wastewater treatment plants are mainly composed of suspended solids, microorganisms, and many organic pollutants [1]. In order to remove those pollutants from secondary effluents, membrane-based filtration and separation processes offer several benefits over the conventional treatment technologies, such as coagulation, flocculation, advanced oxidation processes, ion exchange, activated carbon adsorption [2–4], among others. First, they are effective processes offering high pollutant removal efficiency. Second, there is no need for chemical additives except those required for membrane cleaning. Moreover, filtration units work with lower energy cost, smaller area requirement, are compact in design, and operate easier than other traditional methods. In this perspective, porous ceramic membranes have attracted great attention, due to their advantages in terms of higher flux, better separation properties and fouling resistance, longer working life, and smaller footprints

compared to the most commonly used polymeric membranes [5–9]. Silicon carbide (SiC) membranes possess all the above mentioned features, together with high mechanical strength, good thermal and chemical resistance, superior hydrothermal stability, therefore, they emerged as excellent porous material among the other ceramic membranes [10–13] being suitable for applications in harsh environments, for example in high temperature and in aggressive chemicals [14,15], where other types of membranes fail. However, there are major challenges that limit the use of SiC membranes in wastewater treatment: (i) their cost due to both the high temperature fabrication processing and the precursors, and (ii) their preparation procedure involving multiple steps. To overcome these challenges and to answer industrial demand, the cost of SiC membranes should be reduced by considering the usage of sustainable and/or cheap materials and by preparing efficient and simplified protocols to fabricate SiC membrane layers.

Up to now, many protocols have been developed in the literature in order to fabricate SiC membrane layers. In general, fabrication of SiC membrane layers follows one of two approaches: (i) deposition of pre-ceramic polymers as a precursor for SiC on the surface of macroporous

---

ceramic supports followed by pyrolysis in an inert atmosphere environment and, (ii) deposition of SiC slurry prepared from SiC particles dispersed in alcoholic media with a polymer binder followed by sintering at high temperature, procedure known as ceramic processing. In the first methodology usually polycarbosilane (PCS) precursors, such as allylhydrido polycarbosilane (AHPCS), were used to fabricate highly efficient SiC membranes with controlled composition and porosity. Polymeric precursor based SiC membranes developed on SiC supports are mainly reported for gas separation applications due to the dense structure of SiC membranes [16–18]. The first study on the fabrication of PCS derived (containing sub-micrometer SiC fillers) mesoporous SiC membranes on SiC supports for ultrafiltration applications was carried out by König et al. [19]. Regardless of the application, the judicious choice of the coating suspension parameters and pyrolysis conditions heavily influence the quality of the membranes in terms of efficiency.

The second method is the conventional and well-known method for the preparation of SiC membranes. It is a multiple-step process including colloidal suspension preparation, coating, and membrane sintering. In the first step of this method, the homogeneity of the dispersion of different SiC powders is one of the most important parameter to take into account. In general, in the colloidal processing, well-disperse suspensions are prepared by mixing powders in a very high concentration of alcohol. However, this procedure can cause environmental issues deriving from the release of high amount of alcohol into the atmosphere during the drying of the ceramic slurries. A more effective and eco-friendly approach to solve this issue would be the preparation of suspensions in aqueous media, as reported in Ref. [20,21]. In the second step, depending on the desired membrane pore size, multiple layers can be coated on the macroporous SiC support by dip-coating, spin-coating, and slip-casting. At the end of the procedure, as third and last step, high sintering temperatures are required up to 2100 °C to obtain membranes with the desired physical and chemical properties. This last step makes the production cost of SiC membranes very high.

Even though the second method is widely applied by the scientific community and industries, there are only few published works about it when it concerns SiC. Moreover, the use of microfiltration ceramic membranes in order to treat secondary effluents from wastewater treatment plants is quite rare since most of the studies in the literature exclusively focused on the use of polymeric membranes [1,22,23]. Therefore, this study aims to deepen some still unknown aspects of SiC membranes in terms of fabrication and filtration.

In this vein, a detailed study on the fabrication of homogenous and defect-free pure silicon carbide membranes on silicon carbide support by controlling crucial parameters in suspension preparation and ceramic processing was reported in this paper. Specifically, the effect of fine/coarse powder mixing ratio, solid loading, use of α-SiC powders with different particle sizes, and sintering temperature were studied. The morphology of the membrane layers was investigated with scanning electron microscopy (SEM), high-resolution scanning electron microscopy (HR-SEM), and capillary flow porosimetry. The quality of the up-scaled membranes on industrial SiC tubular support was evaluated by measuring their water permeability and their effectiveness to remove suspended solids, volatile suspended solids and to decrease the chemical oxygen demand as well as total organic carbon content in a secondary effluent from a wastewater treatment plant.

## 2. Experimental

### 2.1. Raw materials

Four types of commercially available α-SiC powders with different average particle sizes, expressed as $d_{50}$, were selected as starting materials to prepare membrane layers. The average particle size of the selected fine α-SiC powder is 0.2 μm (Saint-Gobain, Norway) and average particle sizes of the selected coarse α-SiC powders are 0.4 μm (ESK, Germany), 0.6 μm (ESK, Germany), and 0.8 μm (Washington Mills,

Norway). According to suppliers' information the specific surface areas of all the powders are in the range of 13–80 $m^2/g$. A commercial polyelectrolyte Produkt-KV5088 (PKV) from Zschimmer & Schwarz, Germany, was used as a dispersing agent for α-SiC powders, since it is specifically recommended for SiC processing in water. Optapix CS 76, polysaccharide dicarbonic acid polymer, also supplied from Zschimmer & Schwarz, Germany, was chosen as a binder to improve mechanical strength of green body, which is the membrane before the thermal annealing.

### 2.2. Membrane fabrication

Highly porous multi-channeled SiC tubular supports, which consist of 30 cylindrical channels with a 3 mm diameter for each channel, obtained from Liqtech International A/S, were used for coating SiC membrane layers. Their outer diameter and the total length were 25 ± 1 mm and 305 ± 1 mm, respectively. Initial screening of processing parameters was conducted on 50 mm in length multi-channeled SiC model supports due to their easy characterization. Once defined the optimal conditions for the SiC membrane layer preparation, the experiments were performed accordingly on 305 mm in length multi-channeled SiC supports.

Coating suspensions were prepared by using fine and coarse SiC powders, dispersant, binder, and deionized water kept under continuous mechanical stirring with propeller (IKA RW 16). Suspensions prepared with different fine/coarse powder mixing ratio (0 < fine/coarse SiC ≤ 100) and total solid content (16%–24%) contained α-SiC powders with different particle sizes. All suspensions were prepared using the following sequential addition protocol. First, deionized water and required content of PKV were mixed in a beaker, the fine SiC powder ($d_{50} = 0.2$ μm) was then added and the suspension was stabilized for 5 min. Subsequently, if needed, the required amount of PKV was added to the mixture to disperse the coarse SiC powder ($d_{50} = 0.4$ μm, $d_{50} = 0.6$ μm, and $d_{50} = 0.8$ μm) and the suspension was stabilized for 5 min. The pH was maintained at the desired value (pH~10) throughout the process by dropwise addition of 1 M aqueous $NH_3$, if needed. All suspensions were separately poured in polyethylene bottles and milled for 48 h with spherical 9 mm alumina milling beads to ensure homogenization. Alumina beads were selected as milling media for the dispersion of the raw materials to make processing comparable with large scale processing in industry. Possible contamination of SiC powders with aluminium hydroxide assumed negligible based on the results obtained in the previous study of Liden et al. [24], which revealed that to change the surface properties of powders SiC particles should be covered with substantial amount of $Al(OH)_X$. After the homogenization step, suspensions were separately poured in beakers and 1 wt% optapix CS 76 was added to each mixture. The mixtures were further stirred continuously with a magnetic stirrer at room temperature.

The prepared suspensions were deposited by dip-coating on the porous multi-channeled SiC tubular supports using a home-made dip coating set-up. The dip-coating method is described in detail elsewhere [25]. Briefly, the SiC support were dipped into suspension for 30 s and then pulled out from the suspension at a controlled speed. The membranes, afterwards, were dried at 40 °C overnight in a laboratory drying cupboard.

Once the membranes were dried, the sintering process took place at three different temperatures, chosen in the range to achieve SiC sintering (1500 °C < T < 1900 °C), for 4 h under argon atmosphere, to find the optimum sintering temperature producing good grain joining and appropriate pore size. Finally, membranes were treated in an air furnace (ELS 1000 S SOB, Helmut Rohde GmbH, Germany) to remove the free carbon eventually formed in the pores.

### 2.3. Characterization of materials and membrane layers

The specific surface areas of the powders were determined by the

low-temperature nitrogen adsorption-desorption method on a Micromeritics ASAP 2020 (Micromeritics, USA) equipment, after outgassing under vacuum (residual pressure $10^{-2}$ mbar) at 300 °C to reach a good cleaning of the surface. Specific surface area was determined by using the Brunauer-Emmett-Teller (BET) model.

X-ray diffraction (XRD) patterns of the SiC starting powders were obtained by an Empyrean diffractometer (PANAnalytical, Netherlands), operated at 45 kV and 40 mA with Cu-Kα radiation ($\lambda = 1.5418$ Å).

Zeta potential (ζ) of the four α-SiC powders was determined with a Zetasizer Nano ZS (Malvern Panalytical Ltd, UK) to observe the influence of the pH and of the dispersant concentration on suspension stability. In the first part of experiments, the solution of SiC in concentration of 0.025 M was prepared in 50 ml distilled water, without addition of dispersing agent. The pH of the suspensions was varied in the acidic-basic range by using 0.1 M HCl or KOH solutions, respectively, measured with a traditional pH-meter (654, Metrohm, Switzerland). In the second part, the same amount of mixture was prepared with dispersing agent ranging from 1 to 3 wt% relatively to the SiC powder amount.

The chemical characterization of the surface of the studied commercial α-SiC powders was performed on a SPECS X-ray photoemission spectroscopy (XPS) equipped with a Phoibos 150 MCD-9 detector (SPECS GmbH, Germany) using monochromatic Alka (1486.6 eV) X-ray source at 100 W and 10 kV. Binding energies (BE) were referenced to Si2p at 284.5 eV.

The thickness and the surface morphology of green bodies and membranes were obtained by a TM-1000 (Hitachi GmbH, Sweden) scanning electron microscopy (SEM), whereas the thickness and the surface morphology of final membranes were characterized by an XB1540 (Zeiss, Germany) high resolution scanning electron microscopy (HR-SEM) and a FlexSEM 1000 (Hitachi GmbH, Sweden). The measurements for thickness were taken from 12 different locations around the membrane and then mean thickness was taken as the averaged value.

The mean pore sizes and pore size distributions of the final membranes were analyzed by a Quantachrome, 3G zh, capillary flow porometry (3P Instruments, Germany). The data were obtained first for the wet run then for the dry run. The pores of the membranes were filled with Porofil™ (fluorinated hydrocarbon) wetting liquid having a surface tension of 16 dyn/cm. The wet curve was obtained by measuring air flow rate through the sample with the pressure increasing. Then, the dry curve was measured by increasing the air pressure through a 25 mm long dry membrane sample.

### 2.4. Membrane filtration and cleaning

Final membranes consisting of SiC particles deposited on multi-channeled SiC tubular supports were checked in filtration tests. A commercial pilot scale filtration set-up so-called Liqtech LabBrain (Liqtech International A/S, Denmark) was used to carry out these experiments. The unit consists of a feed tank, a feed pump, a recirculation pump, and a membrane module as shown schematically in Fig. 1. The membranes were sealed using silicon O-rings and placed in a cross flow stainless-steel module. Pure deionized water and the secondary effluent from Biofos wastewater treatment plant (WWTP) in Avedøre, Denmark, were introduced into the system as feed. First, their permeabilities were measured for pure deionized water in order to evaluate their performances. Pure deionized water experiments were carried out at constant transmembrane pressure of 0.4 bar and a cross flow of 2400 l/h for 10 min. The permeate flux was measured gravimetrically. Membrane permeance was determined by dividing the flux by the transmembrane pressure. Then, 50 L of secondary effluent from WWTP was filtered in order to evaluate membrane performances in terms of removal of suspended solids (SS), volatile suspended solids (VSS), chemical oxygen demand (COD), and total organic carbon (TOC). The feed tank was filled with a fresh 50 L of secondary effluent each time to test new batch of the
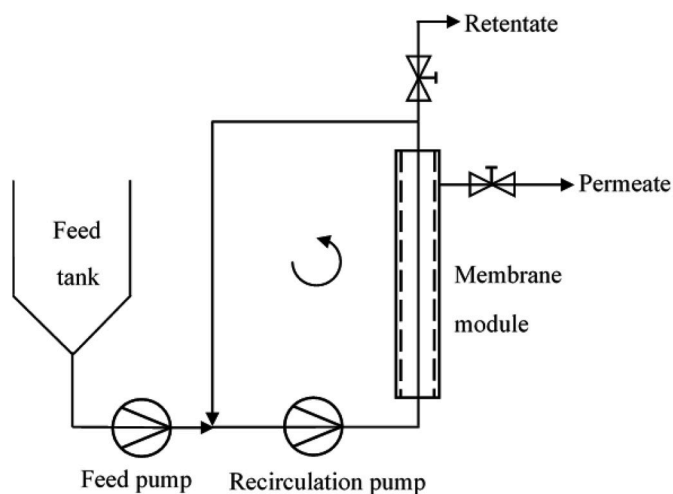


**Fig. 1.** Schematic diagram of cross-flow filtration set-up, Liqtech LabBrain.

membranes and feed sample was not concentrated with membrane filtration. The secondary effluent experiments were run at 250 LMH constant flux, 0.08 bar constant transmembrane pressure, and cross flow of 2400 l/h for 15 min. Recovery factor was set to 90%. Samples from the feed were taken at the beginning of the experiments while samples from membrane permeate were collected at the end of the experiments.

After 15 min of filtration run, each membrane was cleaned chemically. Prior to cleaning with chemicals, membrane was backflushed with permeate water at pressure of 1 bar for 20 s in order to help removing the adhered particles on the membrane surface. Chemical cleaning in place (CIP) were then carried out. Chemicals used for CIP were Ultrasil 75 (Ecolab, Denmark), which is a mixture of nitric acid (10–30%) and phosphoric acid (10–30%), and Ultrasil 115 (Ecolab, Denmark) that consists of potassium hydroxide (10–20%), sodium hydroxide (10–20%), and ethylenediaminetetraacetate (5–10%). The chemical cleaning procedure can be described as follows: 2% w/w of Ultrasil 75 were mixed with distilled water and heated to 40 °C, then the solution was circulated with a cross-flow velocity of 2 m/s for 45 min to drive away inorganic particles. After cleaning with the acid solution, membrane was rinsed with distilled water 2 times at room temperature for 60 s to hinder the generation of poisonous gases during change of chemicals. Afterwards, chemical cleaning solution was prepared from 2% w/w of Ultrasil 115 in distilled water and heated to 40 °C. In order to remove organic particle adhering the porous structure of membrane, the basic solution was circulated with a cross-flow velocity of 2 m/s for 45 min and followed by the 2 times rinsing with distilled water at room temperature for 60 s.

### 2.5. Water analysis

Water samples were collected from both feed and permeate during the filtration studies and they were analyzed for pH, conductivity, turbidity, TSS, VSS, COD, and TOC according to the following Danish standard methods: SS (DS/EN 872: 2005); VSS (DS/EN 872:2005); COD (DS/ISO 15705); TOC (DS/EN 1484:1997). Measurements were repeated three times to assess reproducibility. Conductivities were measured with EC400 model ExStik (Extech, USA) conductivity meter, whereas the pH of both feed and permeate were measured with HQ40D (Hach, USA) pH probe. Turbidities were measured with a turbidimeter TN-100 (Thermo Scientific Eutech, USA). TOC was estimated using TOC analyzer (Hach, USA) and COD was analyzed using AP3900 laboratory robot (Hach, USA). To measure SS, the water sample was filtered through a pre-weighed filter. The residue retained on the filter was dried in an oven at 105 °C for 1 h. After weighing the filter, it was dried again in a muffle furnace at 560 °C for 1 h in order to determine VSS. The SS

and VSS were calculated by the following equations:

$$SS[mg/L] = \frac{([final \ weight \ of \ the \ filter - initial \ weight \ of \ the \ filter])}{volume \ of \ water \ filtered}$$

$$VSS[mg/L] = \frac{([final \ weight \ of \ the \ filter \ with \ SS - final \ weight \ of \ the \ filter \ with \ VSS])}{volume \ of \ water \ filtered}$$

## 3. Results and discussion

### 3.1. Characterization of SiC powders and membrane support

#### 3.1.1. BET and XRD

The different SiC powders are listed in Table 1 with the corresponding particle size and specific surface area declared by suppliers along with data obtained from the $N_2$ adsorption measurements. The specific surface area values given by the supplies show good agreement with the data obtained from the BET evaluations. As expected, the specific surface area decreases when SiC particle size increases. Hereafter, the powders will be referred by using their designation as given in Table 1.

Fig. 2 shows the XRD patterns of the starting SiC powders with different particle sizes. The diffraction peaks are found were found at $2\theta$ = 34, 36, 38, 41.5, 45, 55, 60, 66, 72, 73.5, and 75.5 and correspond to (101), (102), (103), (104), (105), (107), (110), (109), (202), (203), and (204) reflection of the hexagonal α-SiC crystalline structure (6H, α-SiC), respectively [25]. This finding reveals that the four types of starting SiC powders are mainly composed of α-SiC.

#### 3.1.2. Zeta potential and XPS

The stability of a powder suspension critically depends on the surface charge of the particles in aqueous media. ζ-potential measurement is the most common technique for evaluating the surface charge through the measurements of the potential difference between the particles and the layer of ordered fluid molecules surrounding them. ζ-potentials of the four SiC powders as a function of pH without addition of dispersant are shown in Fig. 3a.

The isoelectric point (IEP), i.e. the pH at which the net charge on the particle surface is zero, was measured to be 2.3, 3.3, 3.4, and 3.5 for $SiC_1$, $SiC_2$, $SiC_3$, and $SiC_4$ powders, respectively, in agreement with the presence of thin silica layer at the surface of SiC powders [26,27]. The IEP values of the four SiC powders, therefore, indicate that powders behave like silica in aqueous media. The presence of silica on the powders' surface was further confirmed by the XPS investigation. The XPS spectra of the Si 2p core level for the commercial four α-SiC powders are shown in Fig. 4. Apart from the expected peaks at 102.1 eV associated with Si-C bonds, XPS analysis clearly illustrates the presence of

peaks assignable to Si-O bonds at 104 eV [28,29]. The combined ζ-potential and XPS results suggest a correlation existing between the value of IEP and the amount of the passivating silica layer around the particles with respect to the total mass of the particles. In fact, the lower IEP value is observed for $SiC_1$ sample, which is that with the highest specific surface area, i.e., that made of smallest particles. In this sample the surface passivation brings about the larger amount of silica with respect to the particle mass. Vice versa, the $SiC_4$ sample, showing the lowest specific surface area and made of the largest particles, shows the highest IEP value.

As it can be seen in Fig. 3a, the four SiC powders show almost similar behavior in the acidic-basic range and show a maximum in the ζ-potential values varying between -36 and -44 mV at pH 10. Particles having large ζ-potentials, greater than ±30 mV, are generally considered stably suspended [30]. Thus, it can be inferred that all the SiC powders are well-dispersed and stable at the pH value of 10 and, therefore, this pH was chosen as the working pH in the membrane preparation.

The effect of dispersant content on ζ-potential of SiC powders in aqueous medium was investigated at the selected working pH 10 as shown in Fig. 3b. There is no clear tendency of change in ζ-potential values with increase in dispersant content up to 3 wt%. It seems that it is hard to add extra stability to the dilute suspensions of SiC by adding different amount of dispersant, since all SiC powders are already highly stable at pH value of 10, also in the absence of dispersant. However, the interaction between the particles with an increase in solid loading in the suspension may show different behavior than the diluted suspensions, causing agglomeration but also measurement issues [29,31]. In order to prevent any problem, the addition of 1 wt% of PKV for all four SiC powders was performed during the preparation of suspensions.

#### 3.1.3. Membrane support

Choosing the right support material is the key to prepare high quality membrane layers. The supports having good surface characteristics (smoothness, being defect-free, homogeneity) are desirable for deposition of the membrane layers. Moreover, the support should provide high flux and a strong mechanical support to the membrane layer [16,17].
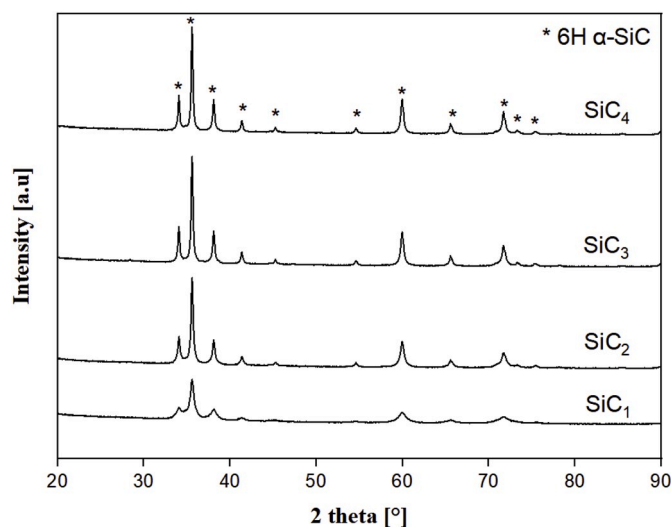


**Fig. 2.** X-ray diffraction patterns of the SiC starting powders with different grain sizes.
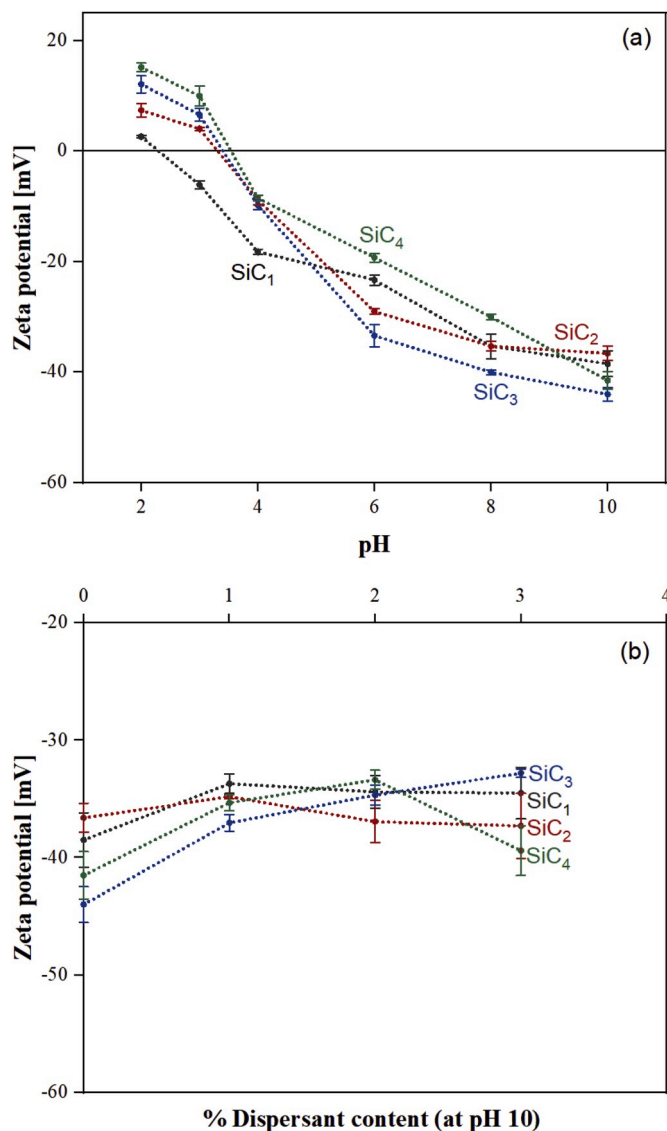
**Table 1**
Powder designation based on their particle sizes and specific surface areas.

| Powder Designation | Particle Size[a] (μm) | Specific Surface Area[a] ($m^2 \ g^{-1}$) | BET Specific Surface Area ($m^2 \ g^{-1}$) |
|---|---|---|---|
| $SiC_1$ | 0.2 | 80 | 77 ± 3 |
| $SiC_2$ | 0.4 | 25 | 24 ± 1 |
| $SiC_3$ | 0.6 | 15 | 13.5 ± 0.6 |
| $SiC_4$ | 0.8 | 13 | 11.8 ± 0.5 |

[a] Data obtained from the suppliers.

**Fig. 4.** XPS spectra of the Si 2p (doublet Si $2p_{3/2}$ – $2p_{1/2}$) core level for the commercial α-SiC powders used in this study.



**Fig. 5.** (a) Virgin multi-channeled SiC support; (b) SEM images of surface of the virgin multi-channeled SiC support.

parameters, possibly affecting the quality of the suspensions, was evaluated. The aqueous suspensions were prepared with different fine/coarse powder mixing ratios and different solid loadings by varying α-SiC powders as listed in Table 2. In order to obtain a membrane layer with smaller interparticle pores, initial aqueous suspensions were prepared by using only fine powder, $SiC_1$, with an increasing amount of solid content. SEM images of the surface layer of green bodies are shown

**Fig. 3.** (a) Zeta potential as a function of pH at the surface of the α-SiC powders without dispersant; (b) Zeta potential as a function of % dispersant content at pH 10.

Keeping in mind the requirements for the selection of support material, a commercially available multi-channeled SiC tubular support was chosen for this work. Fig. 5a shows the multi-channeled SiC tubular support, whereas the SEM surface images are given in Fig. 5b. As shown by SEM images, the microstructure of the support was homogenous and free of macro-defects, such as cracks and pinholes, therefore, suitable to deposit SiC membrane layer on it. According to supplier information the support is highly porous (around 40%) and has high flux. It is also important to note here that the membrane layers were prepared from pure SiC, therefore, being the support and the coating composed of the same material, i.e. having the same thermal expansion coefficient, it is highly probable the membrane layer will not form cracks after deposition on the support [32].

### 3.2. Optimization of suspension and membrane coating

The quality of the membrane layer (to be uniform, homogeneous, defect-free) highly depends on the coating suspension, therefore, optimization of the suspension preparation parameters is another key point to keep in mind. In this vein, the effect of several experimental
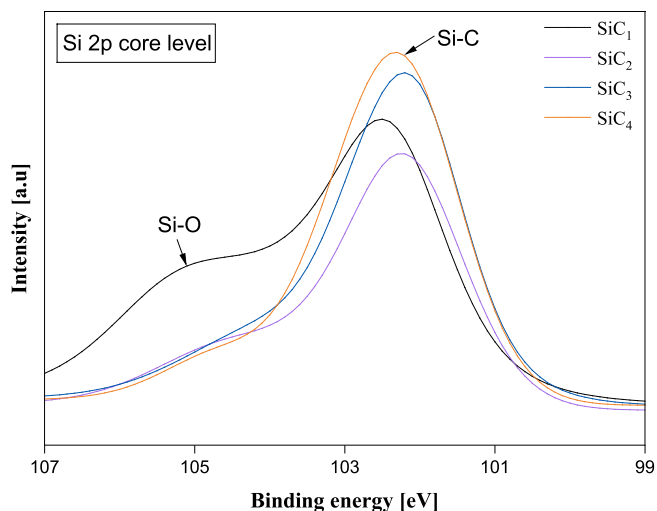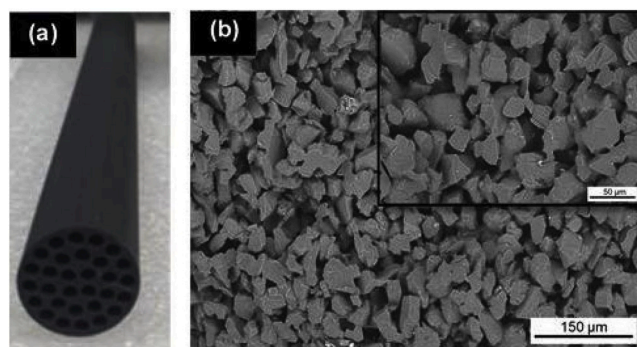
**Table 2**
Membrane designation based on parameters used for optimization of the SiC suspensions.

| Membrane designation | α-SiC powder | Solid loading[a] (wt%) | Powder mixing ratio (%) | Membrane layer quality |
|---|---|---|---|---|
| M1 | $SiC_1$ | L: low | 100/0 | Large cracks |
| M2 | | M: medium | 100/0 | Large cracks |
| M3 | | H: high | 100/0 | Large cracks |
| M4 | $SiC_1$/ | L: low | 50/50 | Large cracks |
| M5 | $SiC_2$ | | 20/80 | Cracks |
| M6 | | M: medium | 50/50 | Large cracks |
| M7 | | | 20/80 | Large cracks |
| M8 | $SiC_1$/ | L: low | 50/50 | Small cracks |
| M9 | $SiC_3$ | | 20/80 | Good |
| M10 | | M: medium | 50/50 | Small cracks |
| M11 | | | 20/80 | Good |
| M12 | $SiC_1$/ $SiC_4$ | M: medium | 20/80 | Good |

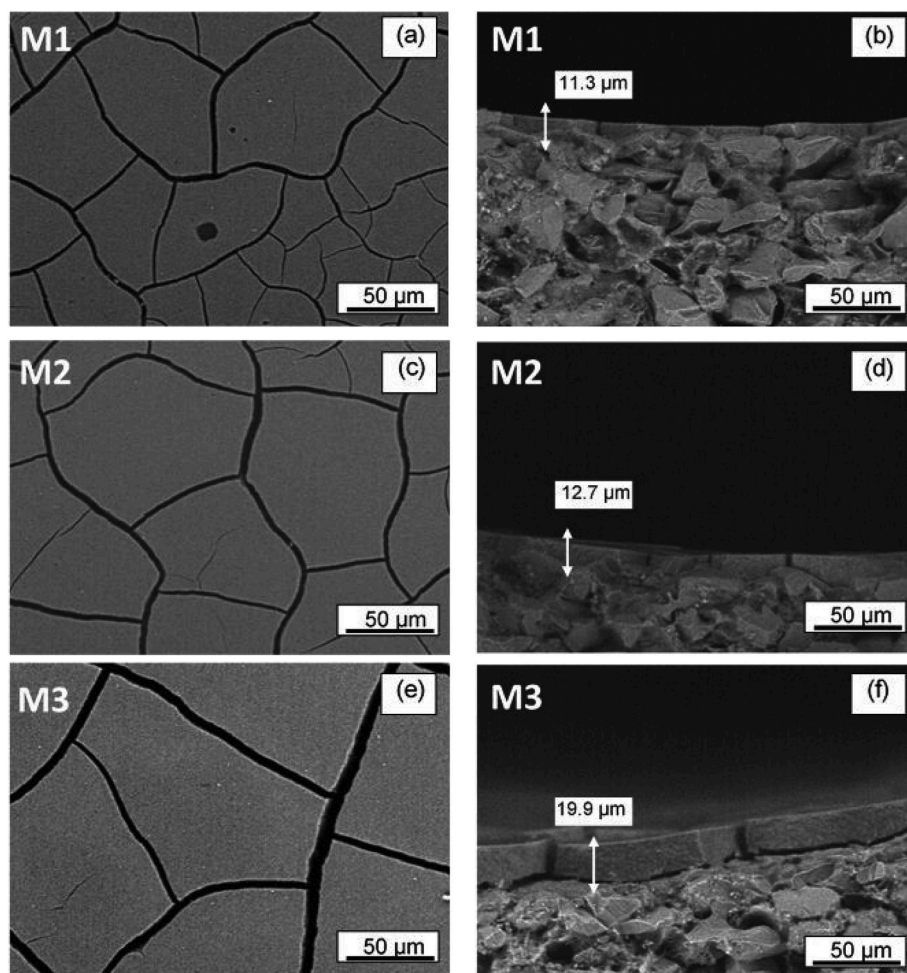[a] Solid loading: 16 wt% ≤ low ≤ 18 wt% ≤ medium ≤ 22 wt% ≤ high ≤ 24 wt%.

**Fig. 6.** SEM images of the surfaces and cross-sections for support with SiC membrane layer prepared from fine powder ($d_{50} = 0.2$ μm): (a, b) low solid content (16 wt% ≤ low ≤ 18 wt%), (c, d) medium solid content (18 wt% ≤ medium ≤ 22 wt%), (e, f) high solid content (22 wt% ≤ high ≤ 24 wt%).

in Fig. 6a, 6c, and 6e, whereas the cross-section images are reported in Fig. 6b, 6d, and 6f. Based on the surface and cross-section SEM images huge cracks and pinholes, even in the case of M1 (low solid content ≤ 18 wt%), were observed on the surface of the membrane layers. It can also be seen that with an increasing solid loading the cracks on the membrane surface are getting bigger, i.e. the crack are bigger in the case of M3 (high solid content ≤ 24 wt% ) compared to M1 (low solid content ≤ 18 wt%) and M2 (medium solid content ≤ 22 wt%). In addition the increase of the solid content causes the detachment of the membrane layer from the support. The thickness of the membranes was estimated to be 11.3 μm, 12.7 μm, and 19.9 μm for low, medium, and high solid content, respectively. This indicates that membrane thickness increases with increasing solid content and when the thickness exceeds a critical value crack formation is energetically favorable [33]. These observations show that it is difficult to fabricate homogenous and defect-free membrane layer by using only fine powder.

Since it was not possible to obtain the desired quality of membrane layers by employing a pure $SiC_1$ powder, the suspensions for the following experiments were prepared using a blend of fine $SiC_1$ powder and coarse α-SiC powders of different particle sizes. In the first set of experiments, $SiC_1$ powder was mixed with $SiC_2$ coarse powder (50/50 by weight) and these suspensions were prepared for low and medium solid contents to prevent crack formation occurring at high solid loading. Fig. 7a and b show the surface images of membranes fabricated using the aforementioned blended suspension. The SEM observations reveal that the surface of support with low solid content was not completely covered, while the membrane with medium solid content formed cracks.

As shown in Fig. 7c and d (surface), a decrease of $SiC_1$ powder down to 20/80 by weight improved the quality of the membrane layer, but the surface of the support was still not completely covered by the SiC particles.

In the second set of the experiments, $SiC_1$ fine powder was blended with $SiC_3$ coarse powder (50/50 and 20/80 by weight). Fig. 7e, 7f, 7g, and 7h present the surface images of the M8, M10, M9, and M11 membranes, respectively. It becomes evident that a decrease of the fine/coarse powder mixing ratio produces a homogenous layer with less fractures at the surface.

Lastly, fine $SiC_1$ powder was mixed with the $SiC_4$ coarse powder. As the previous results showed good membrane quality with medium solid loading and fine/coarse mixing ratio of 20/80 by weight, the last suspension was only prepared following these conditions. As shown in Fig. 8a (surface) and 8b (cross-section), the increase in coarse SiC powder amount allowed to fabricate high-quality membranes with smooth cross-section of homogenous microstructure. M9, M11, and M12 were selected as the best membranes.

Taken together, as described in Table 2, these results give crucial insight into how the morphology of membranes can be improved by optimizing the suspension parameters. The use of blends of SiC powders rather than only one kind of SiC powder increases the quality in the membrane layer as the particles in different sizes pack better together.

### 3.3. Sintering

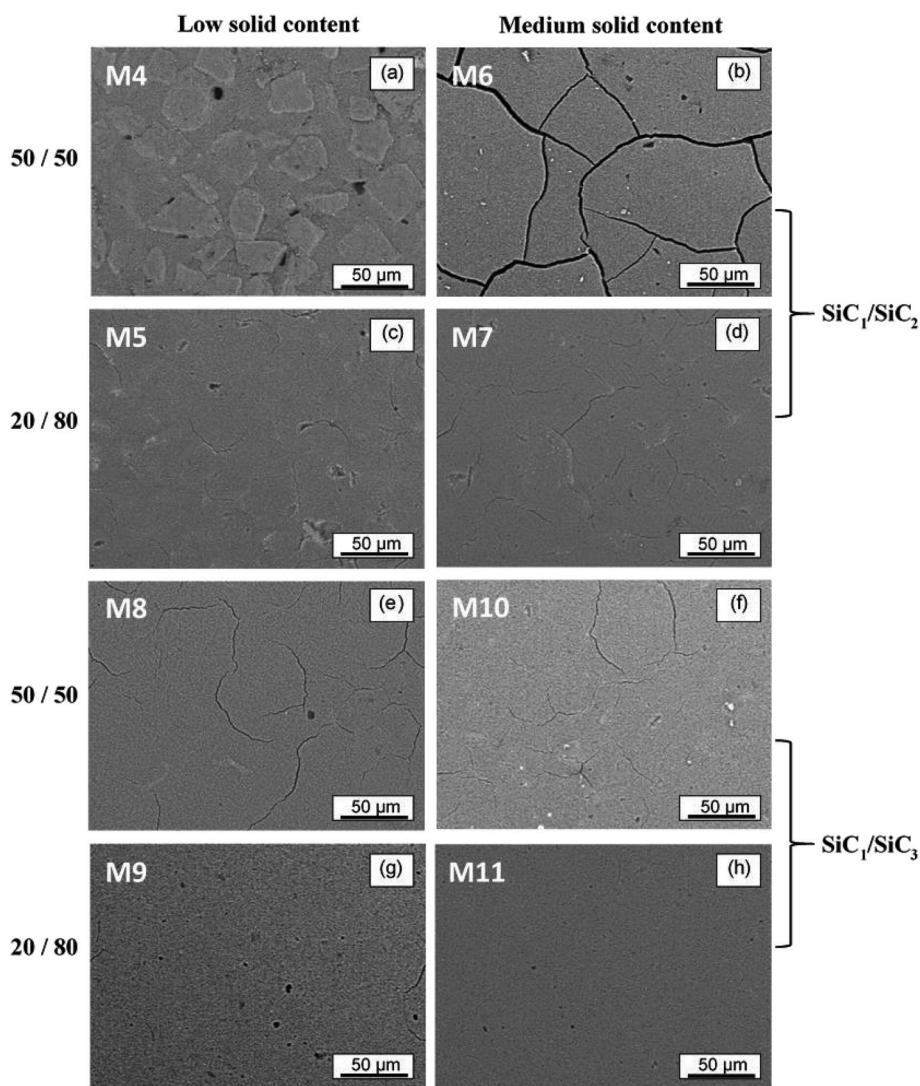Once the suspensions were optimized, the sintering study was

**Fig. 7.** (a, b, c, d) SEM images of the surfaces of SiC membrane layer prepared from $SiC_1/SiC_2$ powders: (a, b) fine/coarse powder mixing ratio 50/50 wt with low and medium solid content, respectively and (c, d) fine/coarse powder mixing ratio 20/80 wt with low and medium solid content, respectively. (e, f, g, h) SEM images of the surfaces of SiC membrane layer prepared from $SiC_1/SiC_3$ powders: (e, f) fine/coarse powder mixing ratio 50/50 wt with low and medium solid content, respectively and (g, h) fine/coarse powder mixing ratio 20/80 wt with low and medium solid content, respectively.
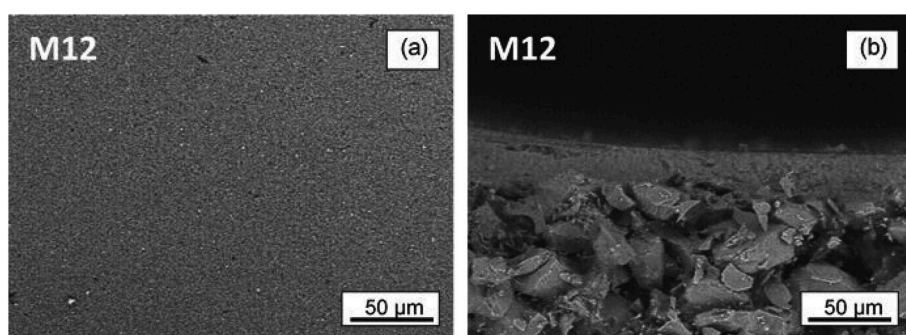


**Fig. 8.** SEM images of the surfaces and cross-sections for support with SiC membrane layer prepared from $SiC_1/SiC_4$ (a, b) fine/coarse powder mixing ratio 20/80 wt with medium solid content.

conducted on the best membranes M9, M11, and M12 for three different temperatures in the range of 1500–1900 °C. The holding time at the corresponding temperature was 4 h for all the samples. For confidentiality reason, hereafter, the highest sintering temperature will be referred as T °C, whereas the other two temperatures will be referred as T-100 °C and T-150 °C, respectively.

The influence of sintering temperature on the structural morphology of the membranes was studied by HR-SEM. Fig. 9 reveals the

microstructure of membrane layers with respect to sintering temperature. At the highest temperature of T °C, the atoms on the surface of fine powders and edge parts of the coarse particles diffused and formed neck regions between the coarse particles by surface diffusion and evaporation/condensation mechanisms causing the disappearance of the small particles in favor of the large particle growth as this process continued. As a result, the big pores start growing at the expenses of the smaller ones. At this temperature, the junction between the grains is clearly
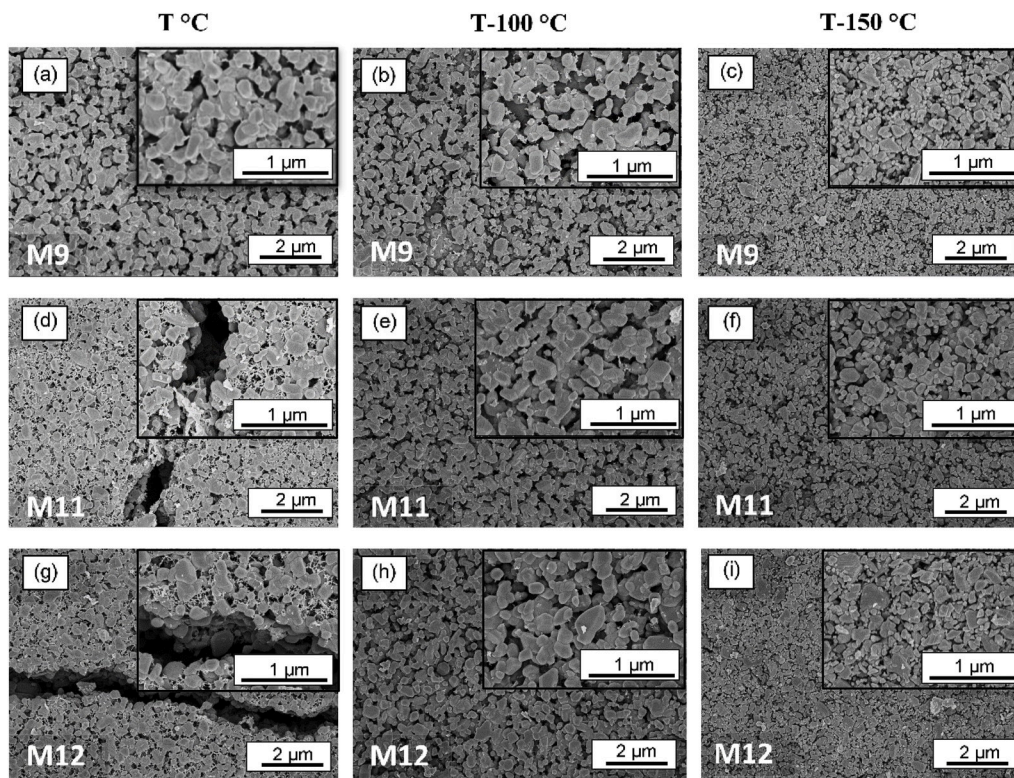
T °C T-100 °C T-150 °C



**Fig. 9.** High resolution SEM images of surface microstructure of the SiC membranes as a function of sintering temperature: (a, b, c) membrane M9 at T °C, T-100 °C, and T-150 °C, respectively; (d, e, f) membrane M11 at T °C, T-100 °C and T-150 °C, respectively; (g, h, i) membrane M12 at T °C, T-100 °C, and T-150 °C, respectively. *: The cobweb structure between the grain of SiC particles in d and g is due to the gold coating of the surface of samples prior to HR-SEM analysis.

visible. For M11 and M12, Fig. 9d and g, the sintering temperature generated some cracks in the layers, probably because the higher solid content used for membrane deposition (compared to M9) causes higher densification of the layer with respect to the green body and, consequently, shrinkage and crack formation. In the case of M9, Fig. 9a, the densification was lower (due to the lower solid loading) and macrodefects could not be observed.

Fig. 9b, 9e, and 9h present the microstructure of the membrane layers at T-100 °C for the three selected membranes. Homogeneous layers with open pores were obtained for the three membranes after sintering. A likely cause of open pore formation may be the absence of the low melting point sintering additives, i.e. metals or metal oxides accelerating the densification of SiC [34,35]. It is also observed that the small and big particles are homogeneously distributed and form a pore network with homogeneous structure. At this temperature the surface diffusion and evaporation-condensation were the predominant mechanisms as well. M12, more than M9 and M11, shows the almost complete disappearance of the small $SiC_1$ particles and a very good joining between large particle. It is possible that this result stems from the particle size difference between fine and coarse SiC powders. In fact, Thomson-Gibbs equation states that larger particles, characterized by a large curvature radius, possess lower surface energy and are more stable than smaller particles (characterized by smaller curvature radius, higher surface energy and lower stability), therefore, larger the particles, faster the evaporation-condensation process that causes the sacrifice of the smaller particles in favor of the larger one growth. Therefore, in M12 formulation and in the presence of the large $SiC_4$ particles, the particle network form earlier than in $SiC_3$-base formulation M9 and M11. In any case, none of the samples form crack at temperature of T-100 °C and it is possible to see the grain joining for three of them, therefore, T-100 °C is an appropriate temperature to avoid shrinkage and crack formation.

When the temperature decreases to T-150 °C, Fig. 9c, 9f, and 9i, neither disappearance of the fine particles nor meaningful joining of

particles were observed. The sintering temperature was not enough to interconnect the small particles together to become relatively larger on the surface. On the other words, there were less microstructural coarsening since the sintering temperature is much lower than T and T-100 °C.

As it can be observed in Fig. 9, an increase in temperature causes the grain growth, consequently, the pore size increases. In all the cases the grains remained equiaxed, as expected for SiC materials due to the stability of α-SiC at high temperatures. These observed equiaxed grains make the SiC membranes stronger [36].

After sintering, in order to remove the residual carbon that may remain in the pores, a surface oxidation step was carried out at a temperature below 800 °C in air atmosphere. No significant difference on the surface morphology was found between sintered and oxidized samples, except some smoothing of surface roughness due to the oxidation step, as visible in the three insets of Fig. 10 providing the images of the surface microstructure of final membranes M9, M11, and M12 sintered at T-100 °C.

The results obtained in the suspension optimization and sintering studies give the boundaries of fabrication of homogenous and defect-free SiC membrane layer. Too high fine powders amount (M1, M2, and M3) or too high fine/coarse SiC powder ratio with low and/or medium solid loading (M4, M5, M6, M7, M8, and M10) for the powders in different particle sizes produced defective membrane layer. All other formulations, as reported in Table 2, gave homogenous and defect-free membrane layer when the sintering took place at T-100 °C for 4 h in an argon environment.

### 3.4. Characterization of up-scaled membranes on SiC industrial support

After successful synthesis of SiC membrane layer on the 50 mm SiC support, the rest of the experiments were carried out using a 305 mm SiC support. The optimum suspension conditions and processing parameters
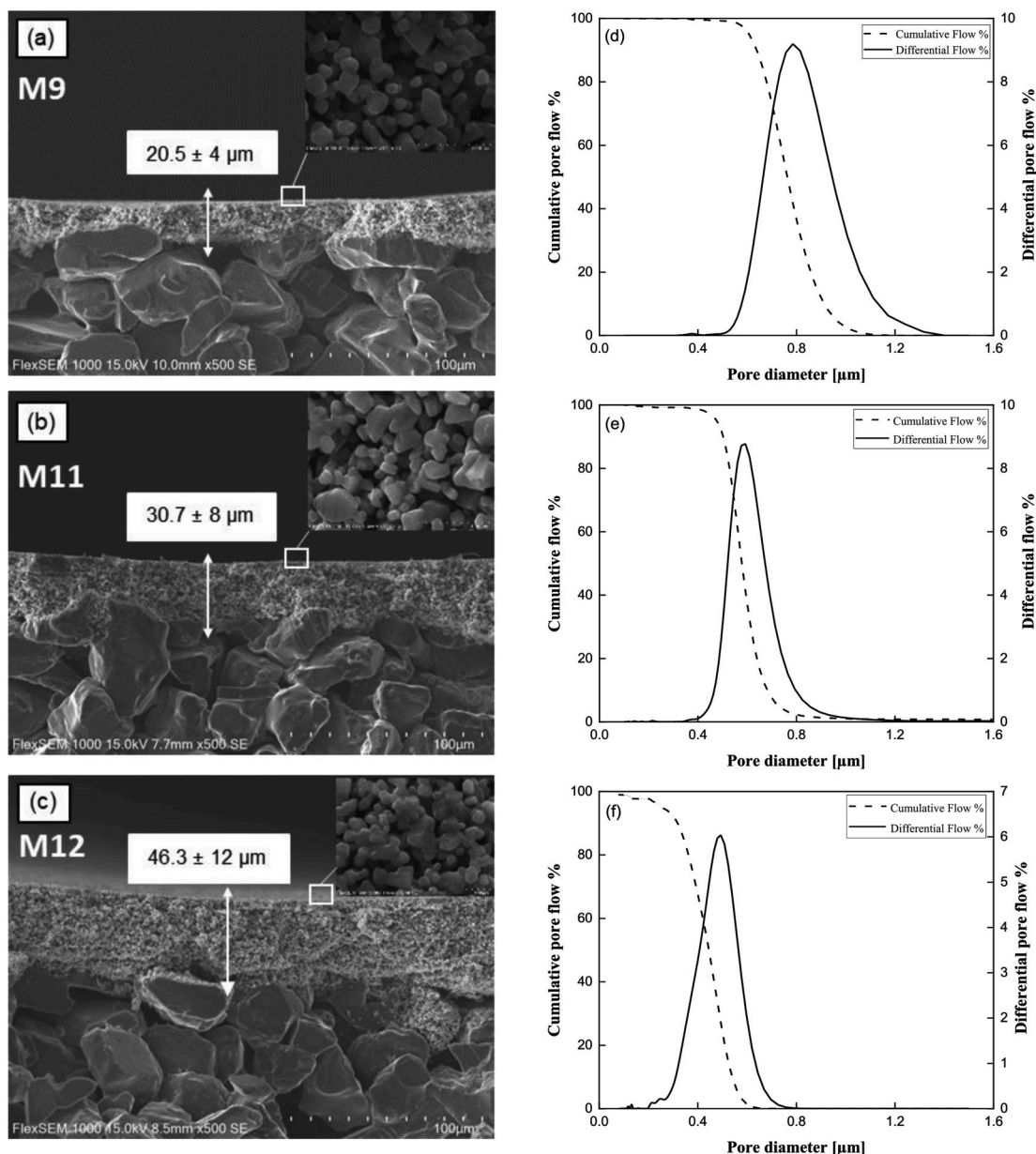
**Fig. 10.** (a, b, c) SEM images of cross-section of final SiC membranes M9, M11, and M12 sintered at T-100 °C, respectively, and (d, e, f) pore size distributions of M9, M11, and M12, respectively.

obtained on 50 mm SiC support successfully worked on 305 mm SiC support, as witnessed by SEM images reported in Fig. 10 (cross-sections and surfaces). Based on the cross-section images, the average thickness of the SiC layer was estimated to be $20.5 \pm 4$ μm for M9, $30.7 \pm 8$ μm for M11, and $46.3 \pm 12$ μm for M12, as expected considering the differences in the used solid content and in fine/coarse mixing ratio. Moreover, the infiltration of the SiC membrane layers in the macropores of SiC supports is not observed, probably due to the correct selection of binder type or the use of optimum binder amount respect to SiC powder amount.

Fig. 10d, 10e, and 10f show the pore size distribution curves of the selective layers of M9, M11, and M12, respectively, for temperature of T-100 °C. The pore sizes of the membranes on the maximum of the distribution curves were 0.75, 0.57, and 0.44 μm for M9, M11, and M12, respectively. In order to verify reproducibility, three independent samples of each membrane type were analyzed. In case of M11 and M12, the mean pore size values had a standart deviation ≤ 6% and for M9 ≤ 19%. As shown in Fig. 10d, M9 membrane had a wide pore size distribution

from 0.4 μm to 1.4 μm. In the case of M11, Fig. 10e, the pore size distribution is sharper than M9 and includes pores up to 1.2 μm. When looking at the graph for M12, Fig. 10f, a narrower pore size distribution was observed compared to M9 and M11. The pores are in the range of 0.2–0.8 μm. It is possible to further confirm what concluded in section 3.3: smaller pores formed when blend of small particles, $SiC_1$, and big particles, $SiC_4$, were used, as a consequence of the disappearance of the smaller particles followed by a joining of the others.

### 3.5. Membrane filtration

Filtration tests were conducted on a cross-flow membrane module by filtering deionized water and the secondary effluent from a WWTP. First, the permeabilities of silicon carbide support and final membranes (M9, M11, and M12) were measured for deionized water. The deionized water permeability of SiC support was found as $12000 \pm 372$ L h m$^{-2}$ bar$^{-1}$, which shows good agreement with the data obtained from the supplier, and permeabilities of final SiC membranes coated on multi-
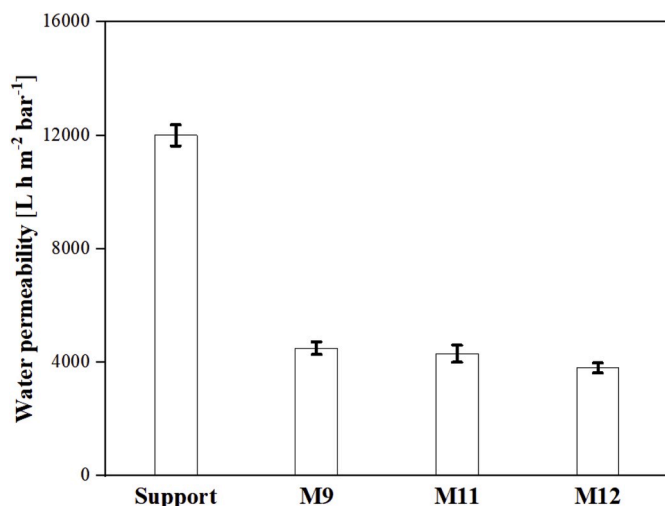
**Fig. 11.** Pure deionized water permeance for SiC support and for the membranes M9, M11, and M12.

channeled SiC tubular support were measured as $4500 \pm 226$, $4300 \pm 300$, $3800 \pm 173$ L h m$^{-2}$ bar$^{-1}$ for M9, M11, and M12, respectively as given in Fig. 11. Water permeability of the support was lowered to 32–38% after deposition of membrane layer. Moreover, water permeability decreases with increasing membrane layer thickness. As an example, the permeability obtained when using the thickest membrane M12 (46.3 μm) is approximately 16% lower than that of the thinnest membrane M9 (20.5 μm).

Second, the intrinsic properties of as-prepared membranes, M9, M11, and M12, were evaluated by filtering the secondary effluent from a WWTP. The data shown in Table 3 indicate the characteristic of the secondary effluent before and after filtration using the three selected best membranes in terms of pH, turbidity, conductivity, suspended solids, volatile suspended solids, chemical oxygen demand, and total organic carbon. Reproducibility of the permeate water quality was investigated by analyzing three samples for each method.

No significant change was found in pH and conductivity values after filtration using M9, M11, and M12 membranes. One unexpected finding was the difference between the feed water characteristic. This difference becomes evident when looking at the drastic increase of SS and COD values in the feed samples between M9 to M12 membranes. In the case of M9, SS value (~2.5 mg/L) and COD value (~24.8 mg/L) indicate that the feed water is secondary effluent, whilst in the case of M12 SS value (~167.38 mg/L) and COD value (~119 mg/L) show that the feed water is mixture of primary and secondary effluents. The observed composition change in the feed samples could be ascribed to pumping of wastewater into secondary effluent by the WWTP from time to time. Since the filtration experiments were performed at different periods using fresh feed water for M9, M11, and M12, the change in the feed concentration was not surprising. The percentage removal of SS, VSS, COD, TOC, and turbidity obtained using M9, M11, and M12 was shown in Table 4. The percentage removal for the specific case of COD was

**Table 4**
Percentage removals of SS, VSS, COD, TOC, and turbidity by membrane filtration of the secondary effluent from a WWTP using M9, M11, and M12.

| Membrane | Turbidity | % Removal of | | | |
| --- | --- | --- | --- | --- | --- |
| | | SS | VSS | COD | TOC |
| M9 | 91 | 75.6 | 91.7 | 2.8 | 4.6 |
| M11 | 94 | 94.0 | 95.3 | 61.3 | 0.73 |
| M12 | 96 | 99.4 | 99.7 | 83.0 | 65.63 |

defined by:

$$\% \text{ COD (removal)} = \frac{\text{COD}_{\text{feed}} - \text{COD}_{\text{permeate}}}{\text{COD}_{\text{feed}}}$$

Similar equations were used for the percentage removal of SS, VSS, TOC, and turbidity. High removal of SS (~94%) and VSS (~95.3%) for M11 and near complete removal of SS (~99%) and VSS (~99.7%) for M12 were observed. Moreover, a significant reduction of COD (~61.3%) for M11 and (~83%) for M12 were observed. The COD removal efficiency for those two membranes was higher than those observed for two different pure SiC membranes manufactured by Liqtech [37]. Similar behaviors were obtained for M11 and M12 since their pore sizes are very similar. These findings support the conclusion that these two membranes, M11 and M12, are optimal for removing SS and reducing COD in wastewater. However, the behavior of M9 was different with respect to that of M11 and M12: the removal efficiencies of SS (~75.6%), VSS (~91.7%) as well as COD (~2.8%) were relatively lower than M11 and M12 ones. A possible explanation for this result could be the greater pore size distribution of M9 respect to M11 and M12. Furthermore, higher removal of colloidal content of the feed samples, manifested as the turbidity, was observed for M11 and M12 rather than M9. The percentage removal of turbidities followed the sequence 96% > 94% > 91% for M12, M11, and M9, respectively.

Kumar and Roy have studied [38] the removal of TSS, COD and turbidity of the sewage effluents by dead-end filtration using two types of alumina ceramic membranes with disc geometry having a pore size of 0.2 μm and 0.45 μm at 0.5–2.1 bar transmembrane pressure. With alumina membrane having pore size of 0.2 μm, they achieved 100%, 85.6%, and 95.5% removal of TSS, COD, and turbidity, respectively. In the case of 0.45 μm, the removal efficiencies were 77.7%, 71.4%, and 82.4% for TSS, COD, and turbidity, respectively. Although the pore size value of M12 membrane developed in this study was greater than those of alumina membranes, better performance was obtained with M12 in terms of TSS, COD, and turbidity removal. Acero et al. have reported a detailed study [3] on different commercial polymeric ultrafiltration and nanofiltration membranes for the treatment of secondary effluents from a municipal WWTP located in Mostoles (Madrid, Spain). The obtained results for the reduction of COD and removal of turbidity for all ultrafiltration polymeric membranes show lower removal efficiency than M12. However, in order to fully compare the performance of different types of membrane to treat real secondary effluents more systematic studies over longer operation periods are necessary.

In summary, membrane M11 and M12 exhibit better performance in terms of removing suspended solids and colloidal particles along with

**Table 3**
Characteristic of the secondary effluent before and after filtration of the final membranes at 250 L h m$^{-2}$ flux and 0.08 bar of transmembrane pressure.

| Parameters | Units | M9 | | M11 | | M12 | |
| --- | --- | --- | --- | --- | --- | --- | --- |
| | | Feed | Permeate | Feed | Permeate | Feed | Permeate |
| pH | – | 7.39 | 7.89 ± 0.29 | 7.11 | 7.45 ± 0.29 | 7.99 | 7.87 ± 0.11 |
| Turbidity | NTU | 10.36 | 0.91 ± 0.25 | 9.28 | 0.58 ± 0.22 | 11.87 | 0.46 ± 0.07 |
| Conductivity | μS/m | 2.74 | 2.68 ± 0.06 | 2.44 | 2.53 ± 0.11 | 2.16 | 2.43 ± 0.03 |
| SS | mg/L | 2.5 | 0.61 ± 0.38 | 14.13 | 0.88 ± 0.43 | 167.38 | 0.96 ± 0.29 |
| VSS | mg/L | 1.32 | 0.11 ± 0.19 | 7 | 0.33 ± 0.14 | 65 | 0.17 ± 0.03 |
| COD | mg/L | 24.8 | 24.1 ± 1.2 | 51.2 | 19.83 ± 0.55 | 119 | 20.3 ± 0.30 |
| TOC | mg/L | 10.9 | 10.4 ± 0.17 | 9.67 | 9.60 ± 0.29 | 27.9 | 9.59 ± 0.21 |

reducing chemical oxygen demand concentration effectively from wastewater. The results discussed in this section demonstrate that the three types of pure SiC membranes (M9, M11, and M12) developed in this study are robust enough to change the wastewater quality.

## 4. Conclusions

Pure SiC membranes on macroporous SiC tubular support were fabricated via ceramic processing consisting of the following steps: selection of precursor materials, preparation of stable suspension, de-agglomeration, dip coating, sintering, and oxidation. Moreover, the intrinsic properties of prepared membranes have been evaluated by filtering secondary effluent from a wastewater treatment plant. The following conclusions can be achieved from these investigations:

- The optimization of the coating suspension was obtaining by controlling coating components such as fine/coarse powder mixing ratios, solid loadings, and use of α-SiC powders with different particle sizes. The use of blend of SiC powders, rather than only one kind of SiC powder, increases the quality of the membrane layer as the particles in different sizes pack better together. The analysis of membrane microstructure indicated high quality, defect free pure SiC membranes were obtained with low-medium solid loadings (in the range of 16–22 wt%) and fine/coarse powder mixing ratio of 20/80 by weight for the mixture of 0.2 and 0.6 μm α-SiC powders as well as mixture of 0.2 and 0.8 μm α-SiC powders.
- The sintering of the deposited layers was studied for three different temperatures in an argon environment. It was found that sintering at T-100 °C (1500 °C < T < 1900 °C) for 4 h was the optimum temperature for the preparation of defect-free SiC membrane layer. The membranes developed in the present study were prepared reducing the sintering temperature with respect to the conventional SiC membrane synthesis. To promote the stability of SiC, the membranes were passivated after sintering by a surface oxidation step in air. This treatment, if carried out below 800 °C, does not cause significant difference on the surface morphology, except some smoothing of surface roughness.
- The prepared novel pure SiC membranes exhibit attractive water permeability and effective removal of particles from the wastewater. The best results in terms of suspended solids, volatile suspended solids, chemical oxygen demand, and colloidal particles removal performance were obtained with the membranes prepared from blended mixture of 0.2 and 0.8 μm SiC powders with medium solid content ($\leq$ 22 wt%) and fine/coarse powder mixing weight ratio of 20/80, having mean pore size of 0.44 μm. These membranes have a potential to be applied in the wastewater treatment since they showed the proper robustness to change the wastewater quality.

This work demonstrates that suspension optimization and coating process parameters heavily influence membrane performance. The procedure here described can be considered a general approach to develop SiC membrane fabrication process and it envisages an easy up-scaling for coating SiC tubular industrial supports for the treatment of wastewater.

## Declaration of competing interest

The authors declare that they have no known competing financial interests or personal relationships that could have appeared to influence the work reported in this paper.

## CRediT authorship contribution statement

**Esra Eray:** Conceptualization, Investigation, Writing - original draft, Writing - review & editing, Project administration. **Vittorio Boffa:** Investigation, Writing - review & editing, Supervision, Funding acquisition. **Mads K. Jørgensen:** Writing - review & editing. **Giuliana Magnacca:** Investigation, Writing - review & editing, Funding acquisition. **Victor M. Candelario:** Conceptualization, Writing - review & editing, Project administration, Supervision, Funding acquisition.

## Acknowledgements

## References

[1] L. Fan, T. Nguyen, F.A. Roddick, J.L. Harris, Low-pressure membrane filtration of secondary effluent in water reuse: Pre-treatment for fouling reduction, J. Membr. Sci. 320 (2008) 135–142, https://doi.org/10.1016/j.memsci.2008.03.058.

[2] C. Reith, B. Birkenhead, Membranes enabling the affordable and cost effective reuse of wastewater as an alternative water source, Desalination 117 (1998) 203–209, https://doi.org/10.1016/S0011-9164(98)00097-6.

[3] J.L. Acero, F.J. Benitez, A.I. Leal, F.J. Real, F. Teva, Membrane filtration technologies applied to municipal secondary effluents for potential reuse, J. Hazard. Mater. 177 (2010) 390–398, https://doi.org/10.1016/j.jhazmat.2009.12.045.

[4] A. Farsi, S.H. Jensen, P. Roslev, V. Boffa, M.L. Christensen, Inorganic membranes for the recovery of effluent from municipal wastewater treatment plants, Ind. Eng. Chem. Res. 54 (2015) 3462–3472, https://doi.org/10.1021/acs.iecr.5b00064.

[5] S.G. Lehman, L. Liu, Application of ceramic membranes with pre-ozonation for treatment of secondary wastewater effluent, Water Res. 43 (2020) 2020–2028, https://doi.org/10.1016/j.watres.2009.02.003.

[6] P.S. Goh, A.F. Ismail, A review on inorganic membranes for desalination and wastewater treatment, Desalination 434 (2018) 60–80, https://doi.org/10.1016/j.desal.2017.07.023.

[7] Z. He, Z. Lyu, Q. Gu, L. Zhang, J. Wang, Ceramic-based membranes for water and wastewater treatment, Colloids Surf., A 578 (2019), 123513, https://doi.org/10.1016/j.colsurfa.2019.05.074.

[8] S. Rezaei, H. Abadi, M. Reza, M. Hemati, F. Rekabdar, T. Mohammadi, Ceramic membrane performance in microfiltration of oily wastewater, Desalination 265 (2011) 222–228, https://doi.org/10.1016/j.desal.2010.07.055.

[9] H. Zhu, X. Wen, X. Huang, Characterization of membrane fouling in a microfiltration ceramic membrane system treating secondary effluent, Desalination 284 (2012) 324–331, https://doi.org/10.1016/j.desal.2011.09.019.

[10] R.J. Ciora, B. Fayyaz, P.K.T. Liu, V. Suwanmethanond, R. Mallada, M. Sahimi, T. T. Tsotsis, Preparation and reactive applications of nanoporous silicon carbide membranes, Chem. Eng. Sci. 59 (2004) 4957–4965, https://doi.org/10.1016/j.ces.2004.07.015.

[11] B. Hofs, J. Ogier, D. Vries, E.F. Beerendonk, E.R. Cornelissen, Comparison of ceramic and polymeric membrane permeability and fouling using surface water, Separ. Purif. Technol. 79 (2011) 365–374, https://doi.org/10.1016/j.seppur.2011.03.025.

[12] R. Neufert, M. Moeller, A.K. Bakshi, Dead-end silicon carbide micro-filters for liquid filtration, in: Adv. Bioceram. Porous Ceram. VI, John Wiley & Sons, Ltd, 2013, pp. 113–125, https://doi.org/10.1002/9781118807811.ch10.

[13] M.C. Fraga, S. Sanches, G. Crespo, V.J. Pereira, Assessment of a new silicon carbide tubular honeycomb membrane for treatment of olive mill wastewaters, Membranes (Basel) 7 (2017), https://doi.org/10.3390/membranes7010012.

[14] Z. Li, K. Kusakabe, S. Morooka, Preparation of thermostable amorphous Si-C-O membrane and its application to gas separation at elevated temperature, J. Membr. Sci. 118 (1996) 159–168, https://doi.org/10.1016/0376-7388(96)00086-5.

[15] Z. Li, K. Kusakabe, S. Morooka, Pore structure and permeance of amorphous Si-C-O membranes with high durability at elevated temperature, Separ. Sci. Technol. 32 (1997) 1233–1254, https://doi.org/10.1080/01496399708000958.

[16] B. Elyassi, M. Sahimi, T.T. Tsotsis, Silicon carbide membranes for gas separation applications, J. Membr. Sci. 288 (2007) 290–297, https://doi.org/10.1016/j.memsci.2006.11.027.

[17] W. Deng, X. Yu, M. Sahimi, T.T. Tsotsis, Highly permeable porous silicon carbide support tubes for the preparation of nanoporous inorganic membranes, J. Membr. Sci. 451 (2014) 192–204, https://doi.org/10.1016/j.memsci.2013.09.059.

[18] B. Elyassi, W. Deng, M. Sahimi, T.T. Tsotsis, On the use of porous and nonporous fillers in the fabrication of silicon carbide membranes, Ind. Eng. Chem. Res. 52 (2013) 10269–10275, https://doi.org/10.1021/ie401116b.

[19] K. König, V. Boffa, B. Buchbjerg, A. Farsi, M.L. Christensen, G. Magnacca, Y. Yue, One-step deposition of ultrafiltration SiC membranes on macroporous SiC supports, J. Membr. Sci. 472 (2014) 232–240, https://doi.org/10.1016/j.memsci.2014.08.058.

[20] V.M. Candelario, M.I. Nieto, F. Guiberteau, R. Moreno, A.L. Ortiz, Aqueous colloidal processing of SiC with $Y_3Al_5O_{12}$ liquid-phase liquid-phase sintering additives, J. Eur. Ceram. Soc. 33 (2013) 1685–1694, https://doi.org/10.1016/j.jeurceramsoc.2013.01.030.

[21] V.M. Candelario, F. Guiberteau, R. Moreno, A.L. Ortiz, Aqueous colloidal processing of submicrometric SiC plus $Y_3Al_5O_{12}$ with diamond nanoparticles, J. Eur. Ceram. Soc. 33 (2013) 2473–2482, https://doi.org/10.1016/j.jeurceramsoc.2013.04.016.

[22] K. Parameshwaran, A.G. Fane, B.D. Cho, K.J. Kim, Analysis of microfiltration performance with constant flux processing of secondary effluent, Water Res. 35 (2001) 4349–4358, https://doi.org/10.1016/S0043-1354(01)00182-8.

[23] Y. Xiao, X.D. Liu, D.X. Wang, Y.K. Lin, Y.P. Han, X.L. Wang, Feasibility of using an innovative PVDF MF membrane prior to RO for reuse of a secondary municipal effluent, Desalination 311 (2013) 16–23, https://doi.org/10.1016/j.desal.2012.10.022.

[24] E. Lidén, L. Bergström, M. Persson, R. Carlsson, Surface modification and dispersion of silicon nitride and silicon carbide powders, J. Eur. Ceram. Soc. 7 (1991) 361–368, https://doi.org/10.1016/0955-2219(91)90059-9.

[25] B.C. Bonekamp, Preparation of asymmetric ceramic membrane supports by dip-coating, in: Fundam. Inorg. Membr. Sci. Technol, fourth ed., 1996, pp. 141–225. Amsterdam.

[26] R.R. Rao, H.N. Roopa, T.S. Kannan, Effect of pH on the dispersability of SiC powders in aqueous media, Ceram. Int. 8842 (2016) 223–230, https://doi.org/10.1016/S0272-8842(98)00027-3.

[27] G.A. Parks, The isoelectric points of solid oxides, solid hydroxides, and aqueous hydroxo complex systems, Chem. Rev. 65 (1965) 177–198, https://doi.org/10.1021/cr60234a002.

[28] J. Guo, K. Song, B. Wu, X. Zhu, B. Zhang, Y. Shi, Atomically thin SiC nanoparticles obtained via ultrasonic treatment to realize enhanced catalytic alkaline and acidic media, R. Soc. Chem. (2017) 22875–22881, https://doi.org/10.1039/c7ra01701d.

[29] V.M. Candelario, R. Moreno, A.L. Ortiz, Carbon nanotubes prevent the coagulation at high shear rates of aqueous suspensions of equiaxed ceramic nanoparticles, J. Eur. Ceram. Soc. 34 (2014) 555–563, https://doi.org/10.1016/j.jeurceramsoc.2013.09.003.

[30] T. Hofmann, F. von der Kammer, Particles in water: properties and processes, in: John Gregory (Ed.), Angew. Chemie Int. Ed., New York, 2007, p. 3611, https://doi.org/10.1002/anie.200685451.

[31] V.M. Candelario, R. Moreno, Z. Shen, A.L. Ortiz, Aqueous colloidal processing of nano-SiC and its nano-$Y_3Al_5O_{12}$ liquid-phase sintering additives with carbon nanotubes, J. Eur. Ceram. Soc. 35 (2015) 3363–3368, https://doi.org/10.1016/j.jeurceramsoc.2015.05.015.

[32] Y. Zhou, M. Fukushima, H. Miyazaki, Y. Yoshizawa, K. Hirao, Preparation and characterization of tubular porous silicon carbide membrane supports, J. Membr. Sci. 369 (2011) 112–118, https://doi.org/10.1016/j.memsci.2010.11.055.

[33] N.B. Dahotre, T.S. Sudarshan, Intermetallic and Ceramic Coatings, CRC Press, 1999.

[34] M. Fukushima, Y. Zhou, Y. Yoshizawa, Fabrication and microstructural characterization of porous silicon carbide with nano-sized powders, Mater. Sci. Eng. 148 (2008) 211–214, https://doi.org/10.1016/j.mseb.2007.09.026.

[35] X.H. Wang, Y. Hirata, Colloidal processing and mechanical properties of SiC with $Al_2O_3$ and $Y_2O_3$, J. Ceram. Soc. Jpn. 28 (2004) 22–28, https://doi.org/10.2109/jcersj.112.22.

[36] J. Eom, Y. Kim, I. Song, Effects of the initial α-SiC content on the microstructure, mechanical properties, and permeability of macroporous silicon carbide ceramics, J. Eur. Ceram. Soc. 32 (2012) 1283–1290, https://doi.org/10.1016/j.jeurceramsoc.2011.11.040.

[37] M.C. Fraga, S. Sanches, V.J. Pereira, J.G. Crespo, L. Yuan, J. Marcher, M.M. de Yuso, E. Rodríguez-Castellón, J. Benavente, Morphological, chemical surface and filtration characterization of a new silicon carbide membrane, J. Eur. Ceram. Soc. 37 (2017) 899–905, https://doi.org/10.1016/j.jeurceramsoc.2016.10.007.

[38] S.M. Kumar, S. Roy, Recovery of water from sewage effluents using alumina ceramic microfiltration membranes, Separ. Sci. Technol. 43 (2008) 1034–1064, https://doi.org/10.1080/01496390801910187.